Available online at www.sciencedirect.com
ScienceDirect
Journal of Controlled Release 119 (2007) 253–261
journal of controlled release
www.elsevier.com/locate/jconrel

Analysis of sustained-release tablet film coats using terahertz pulsed imaging

L. Ho [a,b,c,*], R. Müller [d], M. Römer [e], K.C. Gordon [f], J. Heinämäki [e], P. Kleinebudde [d], M. Pepper [b,c], T. Rades [a], Y.C. Shen [c], C.J. Strachan [g], P.F. Taday [c], J.A. Zeitler [a,b,c,1]

[a] School of Pharmacy, University of Otago, P.O. Box 56, Dunedin, New Zealand
[b] Cavendish Laboratory, University of Cambridge, Cambridge, CB3 0HE, UK
[c] TeraView Ltd, St. John's Innovation Park, Cambridge, CB4 0WS, UK
[d] Institute of Pharmaceutics and Biopharmaceutics, Heinrich-Heine-University, Universitätsstr.1, Düsseldorf, D-40225, Germany
[e] Division of Pharmaceutical Technology, FI 00014 University of Helsinki, Finland
[f] Department of Chemistry, University of Otago, P.O Box 56, Dunedin, New Zealand
[g] Drug Discovery and Development Technology Centre, University of Helsinki, Finland

Received 7 December 2006; accepted 14 March 2007
Available online 23 March 2007

Abstract

The coating quality of a batch of lab-scale, sustained-release coated tablets was analysed by terahertz pulsed imaging (TPI). Terahertz radiation (2 to 120 cm^{-1}) is particularly interesting for coating analysis as it has the capability to penetrate through most pharmaceutical excipients, and hence allows non-destructive coating analysis. Terahertz pulsed spectroscopy (TPS) was employed for the determination of the terahertz refractive indices (RI) on the respective sustained-release excipients used in this study. The whole surface of ten tablets with 10 mg/cm^2 coating was imaged using the fully-automated TPI imaga2000 system. Multidimensional coating thickness or signal intensity maps were reconstructed for the analysis of coating layer thickness, reproducibility, and uniformity. The results from the TPI measurements were validated with optical microscopy imaging and were found to be in good agreement with this destructive analytical technique. The coating thickness around the central band was generally 33% thinner than that on the tablet surfaces. Bimodal coating thickness distribution was detected in some tablets, with thicker coatings around the edges relative to the centre. Aspects of coating defects along with their site, depth and size were identified with virtual terahertz cross-sections. The inter-day precision of the TPI measurement was found to be within 0.5%.

Keywords: Terahertz pulsed imaging; Film coating; Refractive index; Coating uniformity; Process analytical technology (PAT)

1. Introduction

Despite the ongoing development of more sophisticated solid drug delivery systems, tablets are still by far the most prevalent solid dosage form. Not all active pharmaceutical ingredients (API) inherit favourable physical–chemical characteristics for production, storage and administration, thus require dosage form modifications such as coating. Coating can improve taste, aesthetic appearance or mask odour. In addition to this, tablets are often coated with a therapeutic purpose. For example, enteric coating is used to protect the API against degradation in the stomach and sustained-release coating is used to obtain a desirable API absorption rate, and hence an optimum plasma-release profile [1]. Sustained-release coated tablets used in this paper are designed to maintain the plasma concentration of the API at the therapeutic level for a longer duration, thus minimising dose frequency and adverse drug reactions, and consequently increasing patient compliance. The quality of coating properties such as, layer thickness, uniformity and reproducibility of the tablet coating have direct implications on product performance. Lack of quality resulting in dose failures such as dose dumping may precipitate legal and commercial consequences for the manufacturer. It is hence of great interest

* Corresponding author. School of Pharmacy, University of Otago, P.O. Box 56, Dunedin, New Zealand. Tel.: +44 1223435380; fax: +44 1223435382.
E-mail address: louise.ho@teraview.com (L. Ho).
[1] Present address: Department of Chemical Engineering, University of Cambridge, New Museums Site, Pembroke Street, Cambridge, CB2 3RA, United Kingdom.

0168-3659/$ - see front matter © 2007 Elsevier B.V. All rights reserved.
doi:10.1016/j.jconrel.2007.03.011

for these coating properties to be monitored and controlled during the production process.

Routinely in the pharmaceutical industry, tablet coating is controlled by employing calculations on tablet weight-gain during the coating processes with respect to the amount of coating solution applied. However, weight gain determination does not give information on coating uniformity [2]. Other techniques such as scanning electron microscopy, conventional optical microscopy, and laser induced breakdown spectroscopy may be used but are destructive techniques and consequently difficult to apply in on-line analysis [3]. New developments in scanning electron microscopy do allow the non-destructive characterization of film coatings under environmental conditions, and hence can provide information on certain film coating properties. However, using this technique is not possible to acquire information on the coating layer thickness without sample destruction. Near Infrared (NIR) and Raman analysis have also been employed to analyse coating thickness and variability, however these techniques are often restricted by their need for chemometric models, and provide information biased to the surface of the coating. Moreover, only construction of two dimensional chemical images is within the capability of these techniques [4–7]. Magnetic resonance imaging (MRI) can be used to monitor the diffusion of dissolution medium into coating structures and/or the tablet matrix [8]. Its ability to image liquids makes MRI an excellent tool to perform quantitative *in situ* studies of drug release, disintegration and change in pore size during dissolution [9,10]. Nevertheless due to the short relaxation times of typical pharmaceutical solids, in MRI the signal is only acquired from the liquid thus information of the coating structure or all other solid is obtained indirectly.

To date, terahertz radiation has been established for pharmaceutical applications when used as a spectroscopic technique in polymorph identification and quantification [11–13], phase transition monitoring [14,15], and hydrates recognition [16]. Since various techniques for terahertz pulsed imaging (TPI) were pioneered relatively recently [17,18], the application of terahertz pulsed imaging in the pharmaceutical sciences was only explored in chemical mapping [19,20] and tablet coat imaging [21] thus far. This initial work showed the usefulness of this technique for coating thickness analysis and demonstrated the non-destructive nature of TPI due to its ability to penetrate through most pharmaceutical excipients, yet at the same time resolving internal structure by detecting subtle changes in the refractive index. With the implementation of a six-axis robotic system specifically designed for the fully-automated analysis of pharmaceutical solid dosage forms, imaging in the terahertz range (0.3–3.0 THz or 10–100 cm^{-1}) is now readily available as illustrated by Zeitler et al. [22].

In this study, we demonstrate the capabilities of implementing this automatic, three-dimensional TPI set-up as an analytical tool for tablet coating quality; including coating layer thickness analysis, coating uniformity and product reproducibility. Furthermore, an examination of the day-to-day performance, stability and measurement repeatability of the instrument was also carried out.

2. Materials and methods

2.1. Terahertz pulsed spectroscopy (TPS) and refractive index (RI) measurements

The terahertz RI of the tablet coat was determined using TPS. An accurate terahertz RI was essential for TPI coating quality analysis as this RI was used to determine the thickness of the coating layer. The detection of the signal in TPS is unique compared to most conventional spectroscopic methods in that the electric field of the signal rather than only its amplitude is acquired [23]. As a result, not only the amplitude but also the phase of the signal is measured, allowing the direct determination of the spectral absorption coefficient α and the spectral refractive index n of the sample [24]. The relationship between the electric field and the refractive index is defined as:

$$\left[\frac{E_s}{E_r}\right] = T(n)\exp\left[-\frac{\alpha d}{2} + \frac{in\omega d}{c}\right]$$

where E_s is the electric field induced by the terahertz radiation once transmitted through the sample, and E_r is the electric field induced by reference terahertz transmittance radiation. $T(n)$ is the Fresnel reflection at the sample surface, which relates to the refractive index in air (n_a) and the refractive index of the sample in vacuum (n) by: $4n_a/(n_a+1)^2$. d is sample thickness in cm, c is the speed of light in cm s^{-1} and ω stands for the angular frequency of the radiation and is the equivalent of $2\pi f$ [25].

Solid API and tablet excipients were geometrically-diluted with high density polyethylene (PE, Induchem, Volketwil, Switzerland, particle size <10 μm) at 10 or 20% (w/w) concentrations. These concentrations were chosen to avoid signal saturation, especially closer to the higher wavenumber region where the dynamic range of the instrument decreases. The mixtures were then compressed into 13 mm diameter pellets under 2-ton pressure. These pellets were prepared in triplicate with a weight difference of +/−1 mg. Liquid excipients were measured using a demountable liquid cell (PIKE technologies 162–1100, Madison, USA). Refractive index spectra were generated using a TPS spectra1000 transmission spectrometer (TeraView Ltd, Cambridge, UK) at room temperature. Full details of the current TPS spectra 1000 set up are described elsewhere [25]. Briefly, samples were measured in rapid-scanning mode and referenced against the spectrum of a pure PE pellet for solids, and the dry nitrogen atmosphere in the sampling compartment for liquids. The spectral resolution was 1 cm^{-1} and 1800 scans were co-added to acquire spectra over the range of 2 to 130 cm^{-1}. Blackman-Harris 3-term apodization was applied to Fourier transform the terahertz waveforms of both the sample or reference spectrum. Data was acquired and processed using TPI Spectra Software v1.11.0. The RI was determined as the average of the spectral RI over the bandwidth of the TPI system.

2.2. Terahertz pulsed imaging measurements and data analysis

The imaging set up employed in the TPI imaga2000 system (TeraView, Cambridge, UK) has been previously described

[22]. In brief, to scan all surfaces of the tablet, the process was divided into three stages in which the first tablet surface (a), then the central band, and finally the second tablet surface (b) were scanned. Each scan is a two stage process. In the first step a model of the respective surfaces is generated using a laser gauge located beside the terahertz emitter operating at 670 nm. This surface model is the basis for the subsequent terahertz scan and the construction of a 3D terahertz image. All processes were fully automated and performed with the six-axis, robotic arm; the data was acquired using TPICoatingScan software version 1.4.4. The terahertz mapping was performed in point-to-point scan mode with a step size of 200 μm. The axial resolution in z-direction was about 38 μm [22]. The data was analysed using the TPIviewTVL imaging software (version 2.3.0).

2.3. Sustained-release coated tablets

A random selection of ten 10 mg/cm^2 tablets from a batch of lab-scale, blue, biconvex tablets was used for TPI measurements. These tablets were coated with 10 mg/cm^2 sustained release film coating. The coating process parameters were: 20 rpm drum rotation, 100 Nm^3/h for the inlet air flow, 8 g/min for the coating suspension flow, the inlet air temperature was 41 °C and the outlet air temperature was 57 °C. The coating process took 5 h and 8 min. The composition of the tablet core was 87% w/w Flowlac® (lactose monohydrate), 8% w/w diprophyllin and 5% w/w Kollidon VA 64® (vinylpyrrolidone-vinyl acetate copolymer). The coating solution for the sub-coat and main-coat were as follows: 10% w/w Kollidon VA-64®, 2.4% w/w PEG 600 and 87.6% w/w water for the sub-coat, and 30% w/w Kollicoat SR 30 D® (polyvinyl acetate), 4.95% w/w Kollicoat IR® (polyvinyl alcohol-polyethylene glycol graft copolymer), 1.8% w/w talcum, 0.32% w/w triethylcitrate, 0.045% FD & C blue dye (0.5%), and 62.89% water for the main coat. The 10 mg/cm^2 coated tablets had an average height and diameter of 4.1 mm and of 9.3 mm respectively. The average weight for tablet cores was 252.0 mg and the average weight for 10 mg/cm^2 coated tablets was 287.0 mg (total number of tablets weighed = 1000).

2.4. Microscopy

The validation of TPI image analysis was carried out using a stereo-microscope (MZ 75, Leica Mikrosysteme Vertrieb GmbH, Bensheim, Germany), with an illuminator (KL 1500LDC, Leica) and a digital camera accessory (DC300F, Leica). All cross-sections of the tablet were analysed using imaging software (Leica QWin Standard Y2.8, Leica Microsystems Imaging Solutions Ltd, Cambridge, UK).

3. Results and discussion

3.1. Terahertz refractive index determination of the tablet coat

For an accurate calculation of the coat layer thickness, the RI value of the tablet coat is essential as the coating thickness (d_{coat}) is calculated as $2d_{coat} = \Delta t\, c / n$; where Δt is the delay time between the surface reflection and the reflection from the coating layer interface of the terahertz pulse, c is the speed of light and n is the refractive index of the material the terahertz pulse propagating through. Prior to the determination of the actual RI of the coat, the RI was estimated based on the weight percentage and the RI of each of the components in the coating composition. The RI value for Kollicoat SR 30 D®, Kollicoat IR® and talcum was determined. The remaining water soluble dye and triethylcitrate (plasticiser for polyvinyl acetate) were not included in this estimation as their contribution to the weight gain for the final product were negligible. The terahertz RI measured using TPS are 1.92 for Kollicoat SR 30 D®, 1.47 for Kollicoat IR® and 1.85 for talcum. As for the sub-coat, Kollidon VA 64® has a terahertz RI of 1.64, and the RI of PEG 600 is 1.55. Using these refractive indices with respect to their weight composition, the sub coat is estimated to have an RI of 1.62 while the main coat has an RI of 1.86. The weight of the main coat and sub coat are 33.22 mg and 1.84 mg respectively. Taking this into account the terahertz RI of the overall coating structure is estimated to be 1.85. This is not far from the value determined by measuring the RI of the coating on the tablet (1.87) using an uncoated tablet core as reference. For the remainder of this study, a RI of 1.87 was used for the tablet coat. It should be noted that all RI values were derived with tablets in the dry-state, under nitrogen-purged environment. Whilst the terahertz signal is sensitive to water, care was taken that signal distortion from water for both the sample and the reference were eliminated before measurements were carried out.

3.2. Coating layer thickness measurements

Triplicate measurements were made for all ten tablets investigated by TPI. Due to the non-destructive nature of the technique, all tablets were salvaged for subsequent destructive microscopy measurements. A full scan of a single tablet requires 45 min to complete, with no manual involvement. The fully-automated robotic system ensures the sequential completion of the surface map construction at the laser gauge and the 3D terahertz image construction for both tablet surfaces and the central band. While a detailed coating scan is tailored towards at-line process analysis, a singe-point rapid coating thickness determination is also possible. Each terahertz waveform required for the construction of one voxel in the terahertz 3D tablet image takes under 50 ms to obtain, thus providing potential for application as an on-line analytical tool. The temporal waveform was plotted as terahertz electric field strength against penetration depth into the tablet (Fig. 1). The maximum in the signal at penetration depth of 0 mm corresponds to the reflection of the radiation from the tablet surface. While some radiation is reflected back at the surface, most of the radiation penetrates into the tablet matrix (since most pharmaceutical excipients are semi-transparent to terahertz radiation) and is reflected from any subsequent interface with a change in RI. These reflections constitute the subsequent maxima or minima in the terahertz time-domain waveform at longer delay times (further penetration depths). Due to the refractive index differences ($n_{core} > n_{coating}$), a minimum is

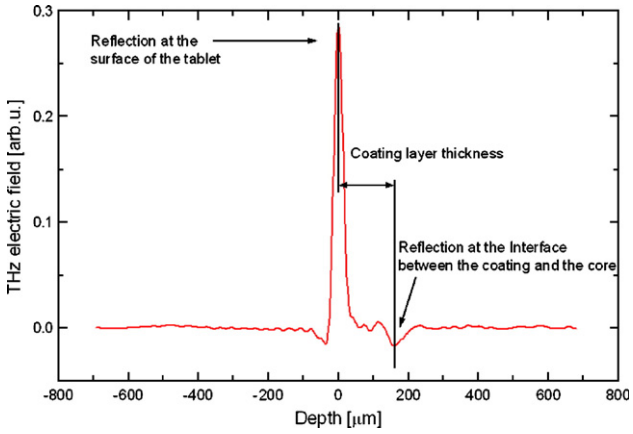

Fig. 1. Typical terahertz waveform from a single pixel of a tablet of the 10 mg/cm^2 batch.

observed which is due to the reflection at the interface between the coating layers and the tablet core. The distance from the maximum to the minimum therefore correlates to the tablet coating layer thickness.

Under the current configuration, the sub-coat layer cannot be temporally resolved in this study. As illustrated previously, the refractive index for the main-coat is higher than that of the sub-coat; resulting in a minimum in the terahertz waveform. The minimum in the signal from the interface between the sub-coat and the main coat cannot be distinguished from the minimum at the interface of the coating structure and the tablet core. As a result, the product of the two minima was a broadened minimum.

Some signal oscillation is observed at 118 μm (Fig. 1). In the terahertz spectral range, a substantial fraction of the radiation is absorbed by crystalline materials at the resonance frequencies of their vibrational modes whilst amorphous materials do not exhibit spectral features at terahertz frequencies and are highly transparent [11]. Most (87%) of the tablet core consists of Flowlac®, a highly amorphous spray-dried lactose α-monohydrate. However Flowlac® contains partly crystalline components that still absorb part of the propagating terahertz radiation. This absorption in the frequency-domain effectively results in oscillations in the time-domain signal. These oscillations in the waveform could potentially distort the signal position and magnitude, but it is obvious from our study that the lactose α-monohydrate signals are weak in comparison to the coat/core interface minimum. The accuracy for the determination the coating layer thickness is therefore not influenced by these oscillations in the time-domain signal. Even for samples with a fully crystalline tablet core, the pulse of terahertz radiation can propagate through the coating structure and advanced data processing can be used to filter out the oscillations from the reflected pulse.

3.3. Tablet surface

After TPI analysis, nine of the ten samples were subjected to microscopy measurements; as one tablet was kept for the investigation of the day-to-day performance stability of the TPI imager. The TPI results show that samples 1, 7 and 9 are 10 μm thinner than the mean coating layer thickness of 142 μm, while samples 5 and 10 are at least 10 μm thicker. This resulting inter-tablet variability at around 7% indicates that the coating reproducibility for this batch is not very high. The TPI coating layer thickness measurements were validated with microscopy results (Fig. 2). Both TPI and microscopy measurement results are normally distributed (Anderson-Darling normality test at significance level $\alpha=0.05$; $P=0.134$ for TPI and 0.813 for microscopy). A two-tailed, paired t-test was performed and a P value of 0.17 was obtained (Table 1). The result of the t-test indicate no significant difference in coating layer thickness between the TPI and microscopy results at significance level $\alpha=0.05$. This shows excellent agreement between the two techniques for coating layer thickness measurements of the same tablets.

In addition to the investigation of inter-tablet coating layer thickness, a comparison of both sides of the tablet surface was made. This comparison shows that some tablets exhibit intra-tablet coating layer thickness variability, where the coating layer thickness on one side of the tablet is up to 10 μm thicker than the other (sample 3). Fig. 3 illustrates the coating layer thickness distribution, presented in histograms, with a mean thickness of 152 μm on one side and 142 μm on the other.

3.4. Central band

The coating layer thickness around the central band for all ten TPI measurements displays a mean batch variability of 6 μm. The largest deviation found was 8 μm less than the mean thickness of 95 μm (sample 7). Compared with the coating layer thickness on the surfaces of the tablet (142 μm), the mean coating layer thickness around the central band was 33% lower

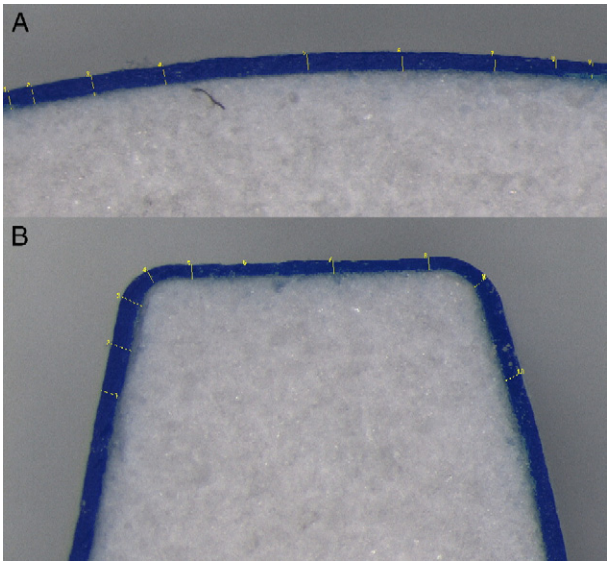

Fig. 2. Light microscopy images used for the validation of coating layer thickens generated with TPI. Coating layer thickness was calculated for tablet surfaces using the yellow calibration bars, these were subsequently analysed using the image analysis software (A). Five calibration bars were used for the coating layer thickness measurement around the central band (B).

Table 1
Optical microscopy validation of TPI coating layer thickness measurements

Sample	Tablet surface microscopy layer thickness (μm)	Tablet surface average layer thickness of all measurements (μm)	Central band microscopy layer thickness (μm)	Central band average layer thickness of all measurements (μm)
S1	139	130	96	88
S3	149	149	102	99
S4	144	143	105	96
S5	160	155	108	101
S6	137	143	91	95
S7	142	130	92	87
S8	150	150	104	100
S9	134	128	89	87
S10	151	152	106	102
t-test (*P* value)	0.17		0.01	

All measurements are in μm. *P* values for *t*-tests on tablet surface and central band measurements are also displayed; where $\alpha = 0.05$.

(Fig. 4). It is possible that these inter and intra-tablet coating thickness inconsistencies may lead to undesirable consequences in formulation performance.

Similar to results on the tablet surfaces, both the TPI and microscopy measurements on the central band also exhibit normal distribution (Anderson–Darling normality test at significance level $\alpha = 0.05$; $P = 0.093$ for TPI and 0.432 for microscopy). A two-tailed, paired t test was performed and a *P* value of 0.01 was calculated (Table 1). This value was below the null hypothesis $\alpha = 0.05$, indicating a difference between the two means in the analysis of coating thickness on the central band. This coating thickness disagreement between the two techniques could be due to the curvature of the central band being much stronger than that of the tablet surfaces. The current configuration of the detector at the TPI setup is optimised for the collection of the reflected light normal to the incident pulse. This is the case with relatively flat surfaces; however surfaces on the central band exhibit significant curvature, and thus some of the light is reflected at angles larger or smaller than 90°, which leads to a slight signal distortion.

In addition to a possible distortion of the signal due to reflection and scattering losses arising from the curved central band, the coating layer thickness discrepancy measured between the two techniques could also be caused by the significant difference in the number of sampling points included into the analysis by the two techniques. For the coating analysis by TPI the layer thickness of more than 1000 pixels over the whole surface area around the central band is measured. The mean layer thickness obtained from the optical microscopy in this study is based on the measurement of five sampling points on the central band per tablet. Due to the destructive nature of the microscopy analysis it is not possible to cut several cross sections through a single tablet and increase the number of data points for the optical analysis. However, the results obtained by

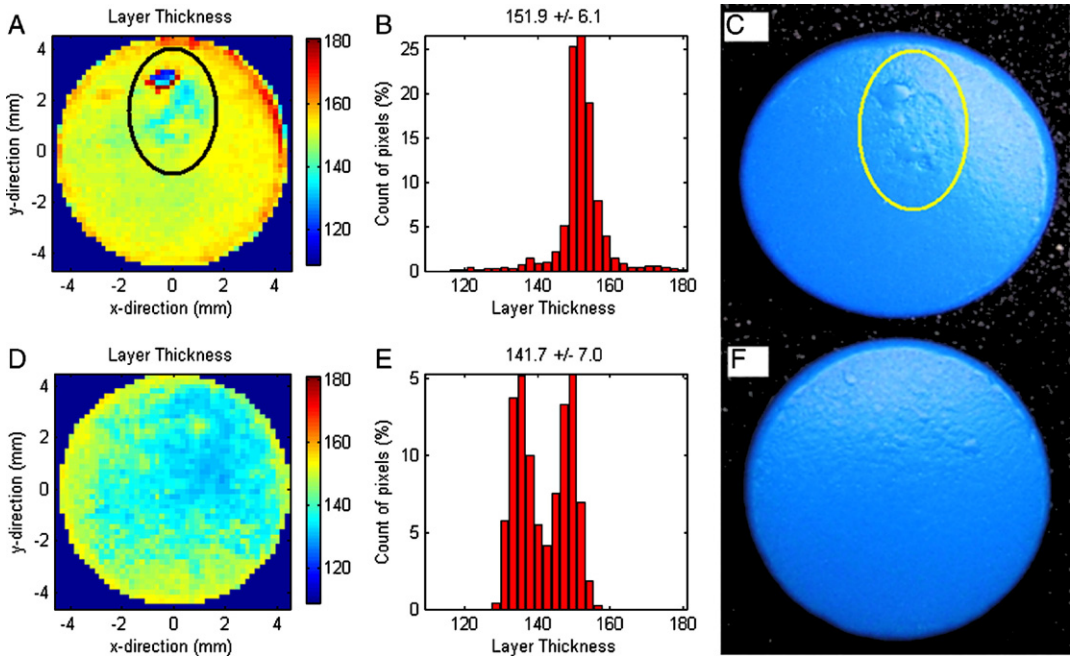

Fig. 3. Sample 3. Defect areas are highlighted by an ellipse in (A) and (C). (A) and (D) are false colour 2D map of the coating layer thickness of tablet side a and b respectively. The units on the colour scale are in μm. (B) and (E) are histograms of the coating layer thickness distribution over the surface of the tablet side a and b respectively. The thickness is in μm. (C) and (F) are photographs of the tablet faces A and B respectively.

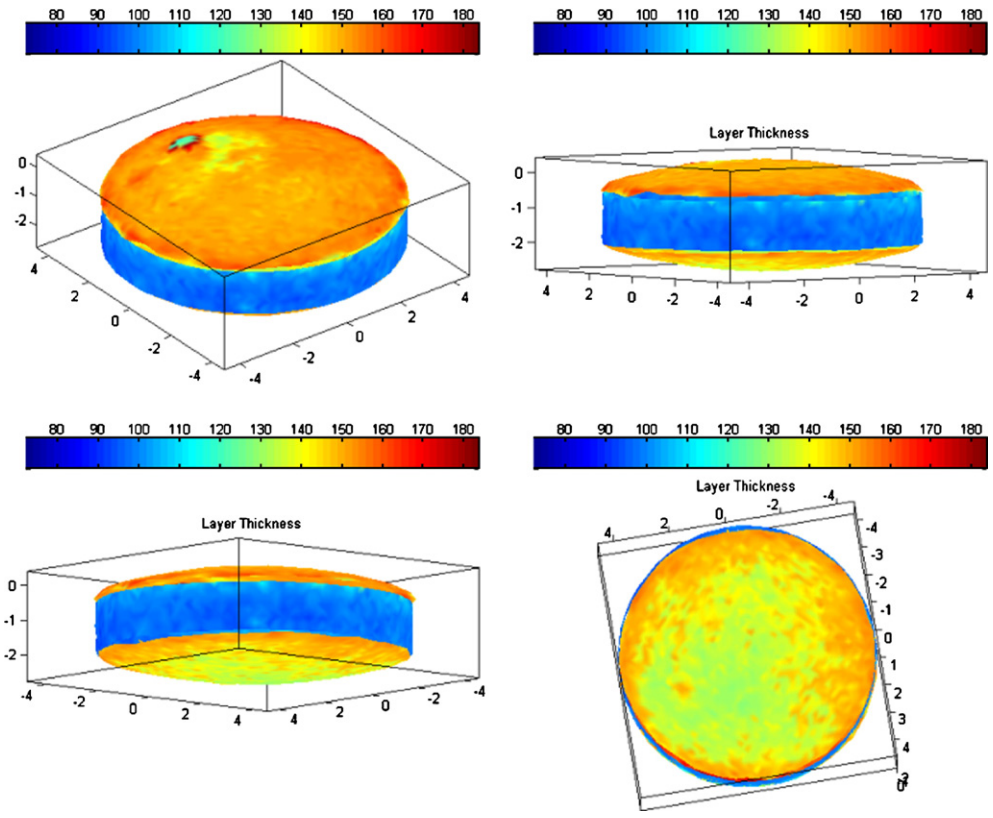

Fig. 4. 3D images of the two tablet surfaces and the central band. The colour coded bar represents coating layer thickness, the scale is in μm. The scales in the *x*, *y* and *z* directions are in mm. The coating layer thickness around the central band is much thinner than that on the surfaces of the tablet.

the optical microscopy layer thickness measurements are all close to or within the range of the histogram distribution from the TPI data.

3.5. Distribution and uniformity

A typical terahertz map of the coating structure over the whole surface of a tablet consists of more than one thousand pixels. This data can be used for a detailed coating distribution and uniformity analysis revealing coating defects and uneven coating distribution invisible to the naked eye.

Sample 3 of the 10 mg/cm^2 coating batch is used as an example for coating distribution and uniformity analysis, since a combination of defects is present on one of the faces of the tablet surface (side a). Cratering is a common coating defect that is observed as a result of insufficient inlet air (drying) temperature or if the spray rate for the coating solution spraying nozzle is too high [26]. The map of the coating layer thickness of the surface of the sample is depicted in C. In this example the coating layer thickness at the crater is 135 μm, 14 μm less than the average thickness observed over the surface of the sample. This crater occupies an area of around 5.8 mm^2 which is more than 8% of the total surface area of this tablet face or about 3% of the surface area of the whole tablet. This example shows the ability of the TPI to assess and quantify the degree of defects in a batch of tablets.

The crater is visible in the false colour terahertz tablet surface map (blue coloured area) along with a blister defect to the left of the crater (red coloured area), where the coating layer is detached from the tablet core (Fig. 3A). The prevalence of blistering, induced by trapped air bubbles underneath or within the coating structure, was relatively low. However, most blisters

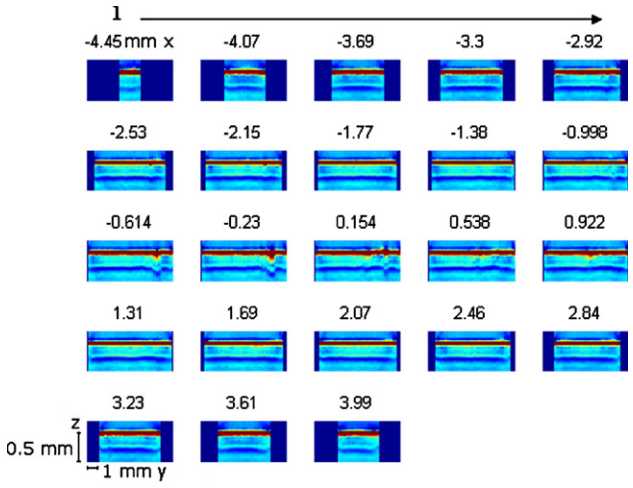

Fig. 5. Virtual cross-sectional images of a 10 mg/cm^2 (sample 3) coated tablets in the *x*-direction. The tablet surface is projected into a plane to facilitate the analysis of the coating structure of the tablet. These virtual cross sections are representations of the terahertz signal relative to the tablet surface, so the area of indentation on the coating/tablet interface (blue band) corresponds to the blister on the coating surface. The blister defect is clearly visible here; it appears on the cross section at −0.614 mm (in the *x*-direction) and spans across the next 3 slides.

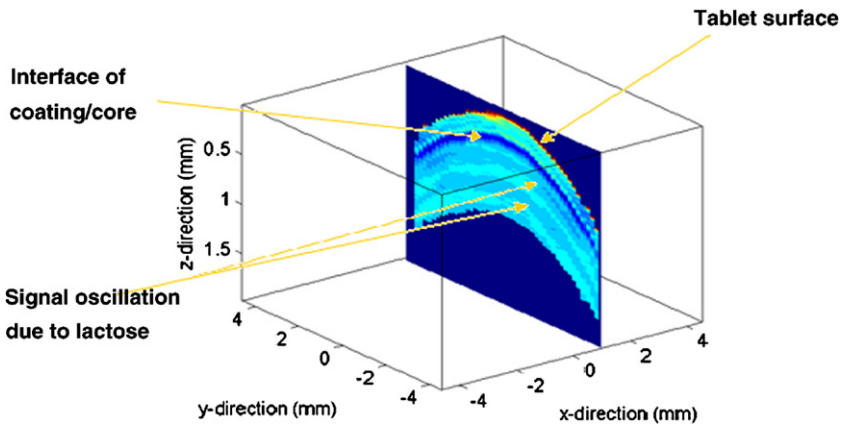

Fig. 6. Virtual cross sections through a 10 mg/cm^2 coated tablet (Sample 3, side a).The air/coating interface is represented in red, and the interface of the coating/tablet core is shown in a darker blue band. This terahertz cross section is presented adopting the curvature of the tablet.

tend to collapse during the coating process. This defect is clearly visible in the virtual cross-sectional images in the x direction in Fig. 5. Virtual cross sections in the *x*, *y* and *z* directions can be generated with any tablet imaged using TPI for close-examination of defect structures. Here, the tablet surface is projected into a plane to facilitate the analysis of the coating structure of the tablet while Fig. 6 shows the typical terahertz cross section using the actual curvature of the tablet. In both figures the air/coating interface is represented in red, and the interface of the coating/tablet core is shown by a darker blue band. Signal oscillation from the partly crystalline lactose in the tablet core leads to some contrast. In Fig. 5, the coating blister slices in the *x*-direction are presented. The blister is visible on the cross section at −0.614 mm and spans across the next 3 slides. These virtual cross sections are representations of the terahertz signal relative to the tablet surface, so the area of indentation on the coating/tablet interface (blue band) corresponds to the blister on the coating surface. These images also provide information about the position of the blister. It is located at 3.84 mm from one end of the tablet and with a diameter of 0.7 mm across the *x*-direction. Using the information from cross-section images in all three directions (*x*, *y* and *z*) the exact location of the defect can be determined. A series of cross-sectional images in the *z*-direction allows the identification of coating defects buried under the outer surface together with its exact depth and location. In Fig. 7, 20 slices in the *z*-direction are plotted where the first slice at 0.0248 mm represents the surface of the coating. The terahertz images indicate that the defect from the blister is extending 314 μm beneath the surface of the tablet.

Coating surface roughness is another coating defect identified in this study (Fig. 8). The coated tablet surface of tablet 3, surface side b has a representation similar to orange skin, thus the coinage of the term ‘orange peel’ defect [27,28].

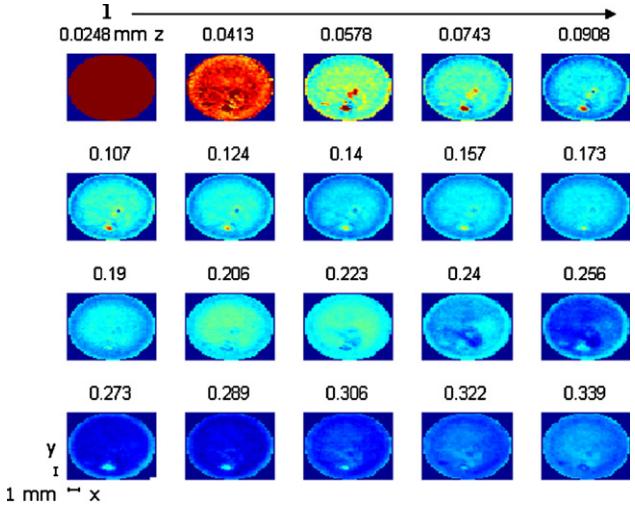

Fig. 7. Virtual cross-sectional images of a 10 mg/cm^2 coated tablets in the *z*-direction. Surface of the tablet projected into a plane; buried structures are relative to the tablet surface. The first slice represents the tablet coating surface at 0.0248 mm.

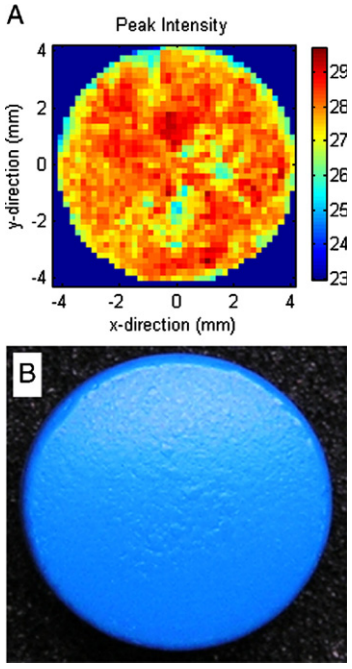

Fig. 8. (A) Terahertz 2D peak intensity map of 10 mg/cm^2 sample 4, tablet surface side b, and its photograph (B). Orange-peel defects in (B) is detected and re-constructed in (A).

Though this defect mainly manifests itself as a non-glossy aesthetically unpleasing area, it may also have implications during the packaging processes. A rougher surface results in high-speed packaging difficulties. Surface roughness can result from pre-existing surface roughness of the tablet core, an unsuitable viscosity of the coating solution, mechanical stress from the coating processes or a combination of the above [26]. TPI can be used to detect surface coating roughness by analyzing the intensity of the light reflected off the coating surface compared to the incident intensity. This variation in the signal strength can be used to generate a terahertz peak-intensity surface map of the tablet coating (Fig. 8A). The red regions on the terahertz peak-intensity map represent areas of smooth coating, as the majority of the light emitted was reflected back to the detector. All other colours represent different degrees of surface roughness that leads to scattering of terahertz radiation and a slight change in the refractive index. Depending on the extent of the roughness, the incident terahertz light is scattered by the uneven coating structure instead of being picked up by the detector. This causes lower peak intensity on the 2D map. The degree of reflectivity is positively proportional to the refractive index, and areas of orange-peel are often spots of thicker coating layer. The refractive index is not necessary constant over the whole tablet surface and subtle differences can be caused by variations in coating density amongst other factors. The impact of the change of refractive index on the detection of coating layer thickness is below the resolution limit of the measurement. The thicker the coating layer, the lower the refractive index and these lower areas of reflectivity correspond to the green/blue areas of the 2D terahertz peak intensity map. Surface roughness can be mapped out in the terahertz peak intensity map and the final 2D map resembled a surface exhibiting the features of an orange skin coating defect structure.

Coating thickness defects that are not visible to the naked eye can also be detected by TPI and mapped out in a 2D terahertz layer thickness map. Again, using tablet 3 as an example, tablet surface b exhibits a bimodal distribution of the coating thickness (Fig. 3E). Though this lack of coating uniformity is not obvious to the naked eye, the areas of different thickness can be clearly mapped out in the 2D terahertz map. The areas close to the edges of sample exhibit an average coating thickness of around 148 μm. In contrast, the coating of the central area was distinctively thinner at 130 μm. The same behaviour is observed for both faces of sample 4. Sample 5 tablet surface side a, exhibits a much thicker coating structure towards the edge of the sample; here the coating thickness is about 183 μm as opposed to 156 μm at the centre of the tablet (data not shown).

3.6. TPI measurement repeatability and longer-term performance stability

The short-term repeatability of the TPI measurements was determined from the relative standard deviation of the triplicate measurements for tablet surface side a and b and the central-band separately. This was carried out to ensure tablet coating variability was not introduced into the repeatability calculation.

Table 2
TPI performance stability measured on 9 separate days over a 17-day duration

Days	Tablet surface side a layer thickness (μm)	Tablet surface side b layer thickness (μm)	Central band layer thickness (μm)
1	155	155	103
2	153	153	102
3	154	155	103
4	153	153	102
5	153	154	103
6	153	154	102
7	154	154	103
8	153	154	103
9	155	153	103
Mean	154	154	103
STD	0.8	0.9	0.5
RSTD	0.005	0.006	0.005

A precision within 0.2% for TPI measurement repeatability was achieved.

The long-term performance validation test was carried out by measuring the same 10 mg/cm^2 coated tablet on nine non-consecutive days within a total period of 17 days. A day-to-day measurement precision within 0.5% for tablet surface side a, 0.6% for side b and 0.5% for the central band is observed in these measurements. The results indicate that TPI has a satisfactory long term stability allowing reproducible measurements with a relative standard deviation of 0.5% over 2 weeks (Table 2).

3.7. Practical considerations of coating analysis using terahertz pulsed imaging and scope for future work

The acquisition of the tablet images in this study requires about 45 min for all surfaces of the tablet. This process involves the construction of a 3D tablet surface model before the actual terahertz scan. The acquisition of the surface model takes about 20 min and can be omitted for tablets with identical dimensions, leading to a substantial reduction in data acquisition time during sequential analysis. Further acceleration of the acquisition process can be achieved by optimization of the current instrument configuration. Imaging at terahertz frequencies is a very recent technology and numerous research activities currently focus on alternative approaches for rapid imaging [29].

The coating properties in the dry-state were the subject of this study. It is at this stage still an open ended question, whether the coating properties in the dry-state reflect the performance relevant characteristics of the coating for drug release. The correlation and significance of these defects to the physical performance of the final product however was beyond the scope of this study. Results from preliminary studies indicate a direct correlation of coating layer thickness (derived using TPI) to the dissolution rate [30], yet additional systematic studies are necessary to investigate this issue further.

4. Conclusion

In this study TPI was for the first time taken beyond the proof-of-principle stage and directly employed for the analysis

of tablet coating quality. The technique is attractive in that one TPI measurement affords not only information on the coating layer thickness, but also the coating reproducibility, distribution and uniformity. Due to the non-destructive nature of the TPI measurements, validation by the destructive optical microscopy was possible and good agreement was found. Along with the excellent measurement repeatability this study demonstrates how TPI has potential as a process analytical tool for coating quality control. Further work is required to address the correlation of information provided by TPI images to physical product performance.

References

[1] G.C. Cole, in: G. Cole, J. Hogan, A. Michael (Eds.), Pharmaceutical Coating Technology, Taylor & Francis Ltd, Philadelphia, 1995, pp. 1–5.

[2] J.D. Perez-Ramos, W.P. Findlay, G. Peck, K.R. Morris, Quantitative analysis of film coating in a pan coater based on in-line sensor measurements, Aaps PharmSciTech 6 (1) (2005).

[3] M.D. Mowery, R. Sing, J. Kirsch, A. Razaghi, S. Bechard, R.A. Reed, Rapid at-line analysis of coating thickness and uniformity on tablets using laser induced breakdown spectroscopy, Journal of Pharmaceutical and Biomedical Analysis 28 (5) (2002) 935–943.

[4] J.D. Kirsch, J.K. Drennen, Determination of film-coated tablet parameters by near-infrared spectroscopy, Journal of Pharmaceutical and Biomedical Analysis 13 (10) (1995) 1273–1281.

[5] S. Romero-Torres, J.D. Perez-Ramos, K.R. Morris, E.R. Grant, Raman spectroscopy for tablet coating thickness quantification and coating characterization in the presence of strong fluorescent interference, Journal of Pharmaceutical and Biomedical Analysis 41 (3) (2006) 811–819.

[6] Y. Roggo, N. Jent, A. Edmond, P. Chalus, M. Ulmschneider, Characterizing process effects on pharmaceutical solid forms using near-infrared spectroscopy and infrared imaging, European Journal of Pharmaceutics and Biopharmaceutics 61 (1–2) (2005) 100–110.

[7] S. Romero-Torres, J.D. Perez-Ramos, K.R. Morris, E.R. Grant, Raman spectroscopic measurement of tablet-to-tablet coating variability, Journal of Pharmaceutical and Biomedical Analysis 38 (2) (2005) 270–274.

[8] J.C. Richardson, R.W. Bowtell, K. Mader, C.D. Melia, Pharmaceutical applications of magnetic resonance imaging (MRI), Advanced Drug Delivery Reviews 57 (8) (2005) 1191–1209.

[9] C.A. Fyfe, A.I. Blazek-Welsh, Quantitative NMR imaging study of the mechanism of drug release from swelling hydroxypropylmethylcellulose tablets, Journal of Controlled Release 68 (3) (2000) 313–333.

[10] J.H.P. Collins, L.F. Gladden, I.J. Hardy, M.D. Mantle, Charactersing the Evolution of Porosity during Controlled Drug Release. Applied Magnetic Resonance (in press).

[11] C.J. Strachan, T. Rades, D.A. Newnham, K.C. Gordon, M. Pepper, P.F. Taday, Using terahertz pulsed spectroscopy to study crystallinity of pharmaceutical materials, Chemical Physics Letters 390 (1–3) (2004) 20–24.

[12] P.F. Taday, I.V. Bradley, D.D. Arnone, M. Pepper, Using Terahertz pulse spectroscopy to study the crystalline structure of a drug: a case study of the polymorphs of ranitidine hydrochloride, Journal of Pharmaceutical Sciences 92 (4) (2003) 831–838.

[13] C.J. Strachan, P.F. Taday, D.A. Newnham, K.C. Gordon, J.A. Zeitler, M. Pepper, T. Rades, Using terahertz pulsed spectroscopy to quantify pharmaceutical polymorphism and crystallinity, Journal of Pharmaceutical Sciences 94 (4) (2005) 837–846.

[14] J.A. Zeitler, D.A. Newnham, P.F. Taday, C.J. Strachan, M. Pepper, K.C. Gordon, T. Rades, Temperature dependent terahertz pulsed spectroscopy of carbamazepine, Thermochimica Acta 436 (1–2) (2005) 71–77.

[15] J.A. Zeitler, D.A. Newnham, P.F. Taday, T.L. Threlfall, R.W. Lancaster, R.W. Berg, C.J. Strachan, K.C. Gordon, M. Pepper, T. Rades, Characterisation of temperature induced phase transitions in the five polymorphic forms of sulfathiazole by terahertz pulsed spectroscopy and differential scanning calorimetry, Journal of Pharmaceutical Sciences 95 (11) (2006) 2486–2498.

[16] J.A. Zeitler, K. Kogermann, J. Rantanen, T. Rades, P.F. Taday, M. Pepper, J. Aaltonen, C.J. Strachan, Drug Hydrate Systems and Dehydration Process Studied by Terahertz Pulsed Spectroscopy, International Journal of Pharmaceutics 334 (1–2) (2007) 78–84.

[17] D.M. Mittleman, S. Hunsche, L. Boivin, M.C. Nuss, T-ray tomography, Optics Letters 22 (12) (1997) 904–906.

[18] N. Hasegawa, T. Loffler, M. Thomson, H.G. Roskos, Remote identification of protrusions and dents on surfaces by terahertz reflectometry with spatial beam filtering and out-of-focus detection, Applied Physics Letters 83 (19) (2003) 3996–3998.

[19] Y.C. Shen, P.F. Taday, D.A. Newnham, M. Pepper, Chemical mapping using reflection terahertz pulsed imaging, Semiconductor Science and Technology 20 (7) (2005) S254–S257.

[20] Y.C. Shen, P.F. Taday, D.A. Newnham, M.C. Kemp, M. Pepper, 3D chemical mapping using terahertz pulsed imaging, Proceedings of SPIE-The International Society for Optical Engineering 5727(Terahertz and Gigahertz Electronics and Photonics IV), 2005, pp. 24–31.

[21] A.J. Fitzgerald, B.E. Cole, P.F. Taday, Nondestructive analysis of tablet coating thicknesses using terahertz pulsed imaging, Journal of Pharmaceutical Sciences 94 (1) (2005) 177–183.

[22] J.A. Zeitler, Y. Shen, C. Baker, P.F. Taday, M. Pepper, T. Rades, Analysis of coating structures and interfaces in solid oral dosage forms by three dimensional terahertz pulsed imaging, Journal of Pharmaceutical Sciences 96 (2) (2007) 330–340.

[23] P.Y. Han, M. Tani, M. Usami, S. Kono, R. Kersting, X.C. Zhang, A direct comparison between terahertz time-domain spectroscopy and far-infrared Fourier transform spectroscopy, Journal of Applied Physics 89 (4) (2001) 2357–2359.

[24] P.Y. Han, X.C. Zhang, Free-space coherent broadband terahertz time-domain spectroscopy, Measurement Science & Technology 12 (11) (2001) 1747–1756.

[25] P.F. Taday, D.A. Newnham, Technological advances in terahertz pulsed systems bring far-infrared spectroscopy into the spotlight, Spectroscopy Europe 16 (5) (2004) 20–24.

[26] R.C. Rowe, in: J.W. McGinity (Ed.), Aqueous Polymeric Coatings for Pharmaceutical Dosage Forms, vol. 79, Marcel Dekker, Inc, New York, 1997, pp. 419–440.

[27] G.R.B. Down, The etiology of pinhole and bubble defects in enteric and controlled-release film coatings, Drug Development and Industrial Pharmacy 17 (2) (1991) 309–315.

[28] M.E. Aulton, A.M. Twitchell, in: G. Cole, J. Hogan, M. Aulton (Eds.), Pharmaceutical Coating Technology, Taylor & Francis Ltd, Philadelphia, 1995, pp. 363–408.

[29] K.L. Nguyen, M.L. Johns, L.F. Gladden, C.H. Worrall, P. Alexander, H.E. Beere, M. Pepper, D.A. Ritchie, J. Alton, S. Barbieri, E.H. Linfield, Three-dimensional imaging with a terahertz quantum cascade laser, Optics Express 14 (6) (2006) 2123–2129.

[30] J.A. Spencer, Z. Gao, T. Morre, L.F. Buhse, D.A. Newnham, Y. Shen, A. Portieri, A. Husain, Delayed Release Tablet Dissolution Related to Coating Thickness by Terahertz Pulsed Imge Mapping. Journal of Pharmaceutical Sciences. submitted for publication.